modern air-to-air refueling operations. An additional 3 min are available before the vehicles descent to an altitude of 10,000 ft, which is considered a safe altitude for completion of docking and pulling out of the glide.

Concluding Remarks

An investigation has been made of the general operational and design considerations for an atmospheric rendezvous mode for orbital logistics vehicles that uses fully recoverable vehicle elements. It is concluded that this mode of operation is feasible, and that it would result in reductions in the size of the orbiter and booster stages of the launch vehicle, provide a powered landing with go-around capability for every mission, and achieve additional lateral range performance. A subsonic rendezvous in either a towing or docking mode seems more attractive than the supersonic case. Recovery of the booster stage in a subsonic towing mode seems to offer some advantage in weight reduction and flexibility of operation.

References

[1] Bird, J. D. and Schaezler, D. A., "Aerospace Applications of Atmospheric Rendezvous." AIAA Paper 72-134, San Diego, Calif., 1972.

[2] Quest, R. and Wagner, L. M., "A Shuttle to Fit the Times," *Astronautics and Aeronautics*, Vol. 8, No. 8, Aug. 1970, pp. 36–45.

Current Drainage to a High Voltage Probe in a Dilute Plasma

NORMAN T. GRIER* AND DANIEL J. MCKINZIE JR.†
Lewis Research Center, Cleveland, Ohio

Introduction

SOLAR cell arrays in the kv range are being proposed for power generation on satellites. If the solar cell cover glass or the dielectric material insulating the connecting tabs between solar cells develops holes or cracks, a large drainage current from the ambient plasma may ensue. Cole et al.[1] measured drainage current on the order of milliamps through 0.0254 cm diam. holes in Kapton H polymide films biased up to 3000 v in a 8 km/sec plasma. This paper reports results for electron drainage current through known size holes in three dielectric materials immersed in a 4 km/sec plasma stream. The dielectric materials were a quartz solar cell cover glass, Kapton H polyimide film, and fluorinated ethylene propelene (FEP) type C. The experimental results are compared with results calculated using a computer program developed by Parker.[2–5]

Facility

The dielectrics were placed in a pyrex bell jar (45.7 cm in diam, 76.2 cm long) attached to the side of a large vacuum tank which houses a Kaufman ion thruster generating an argon plasma (Fig. 1). The vacuum tank pressure was approximately 2×10^{-5} torr. The test specimens were mounted on one end of a 3.2 cm-diam. cylindrical pyrex tube. The ammeter used to measure the drainage current was located between the high voltage power supply and the test specimen. The electrical connecting lines and the ammeter were shielded, with the shield at the potential of the test specimen. In all cases the high voltage probe was biased positively with respect to ground.

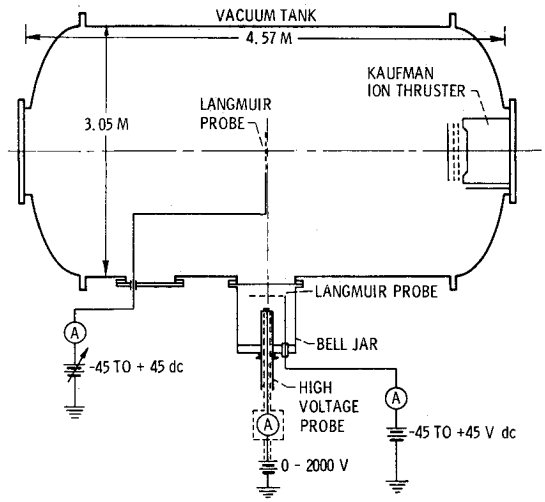

Fig. 1 Sketch of experimental facility (not to scale).

Plasma Diagnostic

Two cylindrical tungsten Langmuir probes and a Faraday cup were used to diagnose the plasma. One of the Langmuir probes (25.4 cm long by 0.0254 cm in diameter) was located on the centerline of the tank at the axial station of the port to the bell jar. The other Langmuir probe (12.4 cm long by 0.0127 cm in diameter) was located in the bell jar approximately 20.32 cm in front of the testing location.

Velocity

On a plane perpendicular to the axis of the tank at the axial position of the bell jar, the ion number density in the ion engine exhaust beam is larger than that in the bell jar. The largest ion density is on the centerline of the beam. A potential difference exists between the engine exhaust beam and the inside of the bell jar. This potential difference accelerates the charge exchange ions in the beam radially. Some of these enter the bell jar along with other scattered ions. The velocity of the ions was calculated from

$$V = (2e\Delta v/M)^{1/2} \tag{1}$$

where Δv is the potential difference between the centerline of the ion engine plasma beam and the plasma potential (assumed constant) in the bell jar determined from the Langmuir probe measurements, and M the mass of the ions.

Number density

The plasma number density in the bell jar was found from $I - v$ characteristic of the Langmuir probe located in the bell jar. For the electron densities expected in the bell jar and the beam, the Debye length is greater than the probe diameter, therefore, a thick sheath is expected about the Langmuir probe. According to electric probe theory,[6] when there is a thick sheath surrounding cylindrical electric probes operating in the electron current saturated region and $ev \gg kT$, the square of the current should vary linearly with the applied

Received January 10, 1972; presented as Paper 72-105 at the AIAA 10th Aerospace Sciences Meeting, San Diego, Calif., January 17–19, 1972; revision received April 3, 1972.

Index categories: Plasma Dynamics and MHD; Spacecraft and Component Ground Testing and Simulation.

* Aerospace Research Engineer.

† Aerospace Research Engineer. Member AIAA.

biased voltage. The number density is related to the slope of this curve by

$$n^2 = (\pi^2/2A^2e^2)(m/e)S \quad (2)$$

where S is the slope, A the probe area, m the electron mass, and e the electronic charge.

Computed Current

Two computer programs developed by Parker[3] were used to predict the current drainage through holes in the dielectric covering of probes which are biased at high voltages relative to the plasma. One of the computer programs solves Vlasov's equation numerically for the current density when the electric field distribution is given. The other program computes the field distribution surrounding a planar probe by solving Laplace's equation numerically. Laplace equation applies where there is no space charge. For an infinite sheath the space charge is zero. Parker[3] shows that maximum current was obtained when the Laplace field rather than the realistic Poisson's field was used to solve Vlasov's equation. Therefore, the Laplace field was used so as to compute the maximum theoretical current through the holes in the dielectrics.

The Laplace field program calculates the field at preselected grid points surrounding an isolated cylinder with a planar probe embedded flush in the center of one of its ends. Cylindrical coordinates are chosen such that the center of the probe has coordinates $z = 0, r = 0$ with the positive z-space above the probe. The size of the probe radius, the cylinder radius and height, grid boundary, and probe voltage, are input data. A dipole law is assumed for the potential between the grid boundary and infinity. In the calculations presented herein the following dimensions were used: probe radius 0.0254 cm, cylinder radius 1.6 cm, cylinder height 3.0 cm, grid radius 50.0 cm, grid distance above cylinder (positive z) 100 cm, and grid distance below cylinder (negative z) 100 cm. The total grid points used were 633 with 594 points in the positive z-space.

The current computer program utilizes the same geometry as the Laplace field computer program. Assuming a Maxwellian gas at infinity, this program numerically computes the current density ratio J/J_0 at the center of the probe for a given field distribution, probe bias voltage, gas temperature at infinity, and directed velocity at infinity. J_0 is the current density for zero bias voltage on the probe. It is given by

$$J_0 = n(kT/2\pi m)^{1/2} \quad (3)$$

where n is the gas number density, T the temperature, and m the mass of the particles. In the tests, the velocity gained by the particles from the probe voltage was much greater than average directed velocity of the plasma. Therefore, the directed velocity at distances far from the probe was assumed zero in the calculations. However, as a check on this assumption, a few cases were computed with a directed velocity of 5 km/sec. There were no changes in the results.

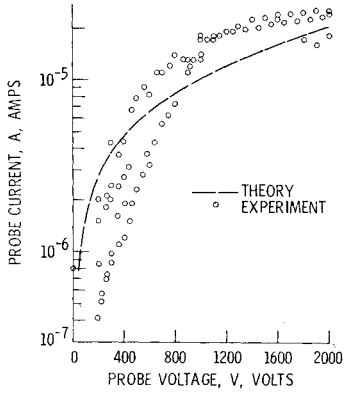

Fig. 2 Probe current as a function of probe voltage for 0.0508-cm-diam hole in Kapton H film.

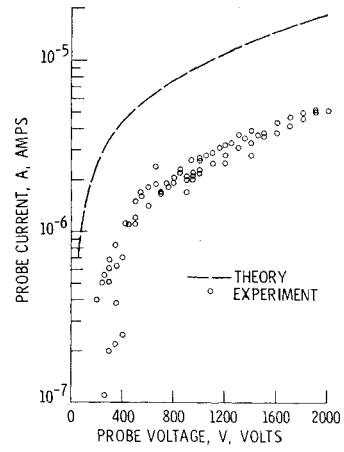

Fig. 3 Probe current as a function of probe voltage for 0.0521-cm-diam hole in FEP, type C.

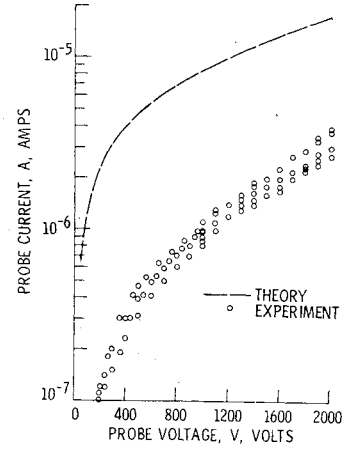

Fig. 4 Probe current as a function of probe voltage for 0.0516-cm-diam hole in quartz.

Results and Discussions

Figures 2, 3, and 4 show the results for the Kapton H film; FEP, type C; and quartz solar cell cover glass; respectively. In Table 1 are listed values for the thickness, hole diameter, and number density used for each specimen. These number densities were determined using Eq. (2) from the experimental saturation electron current of the Langmuir probe in the bell jar. These number densities correspond to an altitude of approximately 300 km. The electron temperature determined from the I-v characteristics of the probe was approximately 3000° K ($\approx$0.3 ev). Since the range of probe potential

Table 1 Test Conditions

Specimen	Thickness, cm	Hole diameter, cm	n, ions/cm^3
Quartz solar cell cover	0.0305	0.0516	1.4×10^6
Kapton H	0.0127	0.0508	1.7
FEP, type C	0.0127	0.0521	1.5

v used was from +20 to +45 V, ev was very much greater than kT in all cases; therefore, thick sheath electric probe theory applied. In determining these number densities from the bell jar Langmuir probe, at least 12 values of the square of the current at applied bias voltages between +20 and +45 V were fitted with a least square linear relation. This gave a rms deviation, for all points, of less than 2%.

From the results presented in these figures, the computed current agrees within a factor of ~3 with that measured for Kapton H. It is larger by approximately a factor of 4 for that obtained with FEP, and larger by approximately a factor of 10 for the quartz measured current, the magnitude being on the order of microamperes. As previously stated, the current calculated using a Laplace field in the space surrounding the hole yields an upper current limit for a planar probe in a plasma. Therefore, the apparent agreement between theory and experiment for Kapton H is probably due to phenomena not considered in the theory. One phenomenon that may enhance the experimentally measured current is sputtering of the dielectric material. Sputtering produces a gas cloud near the hole. As some of the plasma electrons travel toward the hole, they make ionizing collisions with the gas cloud particles creating more electrons. These ejected electrons along with the original electrons now travel toward the hole, thereby enhancing the measured current. If sputtering is present, the results indicate that Kapton H is sputtered the most, FEP next, and quartz is sputtered the least.

Although the magnitude of the computed current differs from the measured current, the variation of the current with voltage is in agreement with experimental trend. This suggests that the theory may be used to estimate the drainage current at higher voltages than those presented here. However, it is expected that sputtering and other effects may become more severe at higher voltages for some materials.

Conclusions

Parker's method for calculating the current through holes in dielectric covering of probes satisfactorily predicts the trends in experimentally measured current in a dilute plasma for voltages up to 2000 V. A Laplace field was used to numerically predict an upper limit for the drainage current. For holes in quartz and FEP, the theoretical current was larger than the measured current for all valtages presented. For Kapton H the theoretical current and the measured current were approximately in agreement over the full range of voltages presented. Since the computed current is the theoretical maximum current, this agreement suggests that other phenomena may be occurring near the hole enhancing the measured current.

References

[1] Cole, R. K., Ogawa, H. S., and Sellen, J. M. Jr., "Operation of Solar Cell arrays in Dilute Streaming Plasmas," TRW-09357-6006-R000, NASA CR-72376, March 15, 1968, TRW Systems, Redondo Beach, Calif.

[2] Parker, L. W. and Whipple, E. C., Jr., "Theory of Spacecraft Sheath Structure, Potential, and Velocity Effects on Ion Measurements by Traps and Mass Spectrometers," *Journal of Geophysical Research*, Vol. 75, No. 25, Sept. 1, 1970, pp. 4720–4733.

[3] Parker, L. W., "Theory of the Circular Planar (Guarding) Langmuir Probe," ERL 100-AL2, Dec. 1968, ESSA, Boulder, Colo.

[4] Parker, L.W., "Theory of Electrostatic Planar and Spherical Probes," CR-704, 1967, NASA.

[5] Parker, L. W. and Whipple, E. C., Jr., "Theory of a Satellite Electrostatic Probe," *Annals of Physics*, Vol. 44, No 1, Aug. 1967, pp. 126–161.

[6] Chen, F. F., "Electric Probes," *Plasma Diagnostic Techniques*, edited by R. H. Huddlestone and S. L. Leonard, Academic Press, New York, 1965, pp. 113–200.

Helium Absorption into Nitrogen Tetroxide (NTO) and Aerozine-50 (A-50)

PHILIP J. KNOWLES*
TRW Systems, Houston, Texas

Nomenclature

A = liquid gas interface area, m²
K_G = mass convection coefficient, moles/hr m² atm
$\dot{N}_c$ = mass convection rate of helium into the propellant, moles/hr
$\dot{N},\dot{N}_0$ = mass convection rate (and at $\theta = 0$), moles/hr
P,P_0 = total pressure of the ullage gas (and at $\theta = 0$), atm
P_s = total pressure of the ullage gases when the propellant is saturated with helium, atm
p = partial pressure of helium above the saturated propellant, atm
R = universal gas constant
V = total volume of the ullage gases, m³
Z = compressibility factor for helium = $P/\rho RT$
δ = partial derivative of
Δ = change of or delta, $\Delta P = P - P_s$
η,η_0 = number of moles of helium gas in the ullage (and at $\theta = 0$)
θ = time, hr

Introduction

THE solubility limits of helium into NTO and A-50 propellants have been identified, but the mechanism describing helium absorption between the limits has not. A simplified, yet unique, analytical technique has been developed and is provided in this note for simulating the absorption phenomena under closed storage conditions. The model developed has been used to evaluate propellant conditions for Apollo missions. A study was initiated to predict Service Propulsion System (SPS) tank pressures because Apollo flight data indicates that ullage pressure decays were a direct result of helium being absorbed into the propellants. The results of this analysis were compared with Apollo 8–12 and 14 flight data and were found to closely agree with the flight data.

Helium Absorption Mechanism

The formulation developed here requires the use of the mass convection analogy, Dalton's law of partial pressures and Henry's law for fluid solubility. This development was initiated by assuming the following. 1) The system was closed; i.e., no flow or leakage exists. 2) All diffusion is normal to the gas/liquid interface. No cross-diffusion or propellant vaporization exists.

$$\dot{N}_c = -K_G A \Delta P \tag{1}$$

mass convection at the interface. 3) The driving force (ΔP) at all times is

$$\Delta P = P - P_s \tag{2}$$

where the saturation pressure (P_s) can be expressed as

$$P_s = p + VP_{\text{propellant}} \tag{3}$$

The concentration (C) of helium in the gas can then be equated to pressure as follows:

$$C = \eta/V = p/(ZRT) \tag{4}$$

For very low absorption rates, the assumptions that the ullage gases are isothermal ($dT = 0$) and that the gas behavior is pseudo-ideal ($dZ = 0$) are justifiable. With these assumptions, the concentration gradient within the ullage can be simply expressed as

$$dC = dp/ZRT \tag{5}$$

Received January 6, 1972; revision received April 17, 1972.
Index category: Properties of Fuels and Propellants.
* Member of the Professional Staff. Member AIAA.